The Modification of Superconductors

PLATINUM GROUP METALS CONFER NOTABLE PROPERTIES

By Yu. M. Shul'ga, E. N. Izakovich, V. I. Rubtsov and B. F. Shklyaruk

Russian Academy of Sciences, Institute of Chemical Physics, Chernogolovka, Russia

Since the discovery of the first high temperature superconductor, YBaCuO, many attempts have been made to improve its properties by the addition of modifiers; indeed almost all of the elements in the Periodic Table have already been tried in this way. The present survey, covering both our own work and the published literature, examines the effects of adding the platinum group metals to the superconductor, resulting in the formation of several new compounds, many of which are semiconducting and some of which may have potential value in engineering and chemical technology. The complex oxides formed are characterised and data on the superconducting properties of the modified YBaCuO oxide phases are presented.

Immediately after the discovery of high temperature superconductors (1) a series of papers appeared discussing their modification by other metals; now almost all the elements of the Periodic Table have been used as modifiers. The aims of this research were as follows: to produce a modification-induced increase in the critical temperature (T_c), to verify the hypothesis on the mechanism of superconductivity by substituting atoms of one type for those of another, to find the effect of additions to the initial mixture on the size of the particles formed, and to increase the rate of formation of the main phase, for example, $YBa_2Cu_3O_{7-\delta}$.

The high reactivity of the components in the superconductor cause it to react with the container material, forming new phases which affect the properties of the superconductor. Such phenomena, observed for the $YBa_2Cu_3O_{7-\delta}$ + platinum metals system, were discussed recently (2). In this review we present data from the literature and from our own work on the interaction of $YBa_2Cu_3O_{7-\delta}$ with all the platinum group metals; and new phases containing platinum metals are characterised.

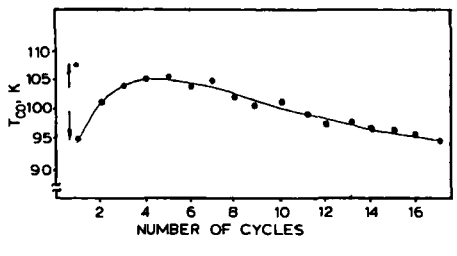

Fig. 1 The dependence of T_{co}, the onset of the superconducting transition temperature, on the number of cooling-heating cycles for $YBa_{1.8}Cu_3Ru_{0.3}O_{7-\delta}$ (sample No. 9, see Table I) is shown. From the second cycle onwards T_c for cooling and heating coincide

The $YBa_2Cu_3O_{7-\delta}$ + Ruthenium System (3)

Compounds of the platinum group metals are known to be catalytically active for redox reactions, with ruthenium exhibiting the highest activity towards inorganic ions (4). In the absence of ruthenium, the synthesis of $YBa_2Cu_3O_{7-\delta}$ usually takes place at 920–950°C and requires about 60 hours (5). However, the Y-Ba-Cu-Ru-O system is characterised by two peculiarities: a shortening of the synthesis time of $YBa_2Cu_3O_{7-\delta}$, by a factor of approximately six, and a decrease in the reaction temperature to 880°C, which can be

Table I

Superconducting Properties of $YBa_xCu_yRu_zO_{7-\delta}$

Sample number	Ru_z	Ba_xCu_y	$T_c(R)$,K		$T_c(\chi)$,K		
			T_{co}	T_c	$T_{c_{0.1}}$	$T_{c_{0.5}}$	$T_{c_{0.9}}$
1	0.1	Ba_2Cu_3	89	–	54	12	2
2		$Ba_2Cu_{2.9}$	100	95	91	78	22
3		$Ba_{1.8}Cu_3$	–	–	48	15	8
4	0.2	$Ba_2Cu_{2.8}$	95	92	88	85	68
5		$Ba_{1.8}Cu_2$	–	–	77	18	5
6		$Ba_{1.8}Cu_{2.9}$	94.5	93	86	78	47
7		$Ba_{1.8}Cu_{2.8}$	95	92	92	75	59
8	0.3	Ba_2Cu_3	88	83.5	86	46	8
9		$Ba_{1.8}Cu_3$	94.5	94	92	86	69
10	0.4	Ba_2Cu_3	85	–	69	64	7
11		$Ba_2Cu_{2.6}$	99	94	87	62	9
12		$Ba_{1.8}Cu_3$	97.5	96	88	81	60
13	0.5	Ba_2Cu_3	92	88.5	87	29	5
14		$Ba_2Cu_{2.5}$	90	89	88	71	16
15		$Ba_{1.8}Cu_3$	94	93	89	88	77
16		$Ba_{1.8}Cu_3$	90	77	79	66	11

explained by assuming that ruthenium acts as a catalyst for the synthesis. It should be noted that an increase in the duration of the synthesis causes degradation of the superconducting properties; thus, sample No. 15, whose composition is presented in Table I, required 10 hours to sinter, whereas sample No. 16 took 26 hours.

From Table I it may be seen that certain specific ratios of barium, ruthenium and copper are required to produce materials having a high superconducting transition temperature, T_c, (see sample Nos. 2, 4, 6–9 and 11–15). The appearance of a superconducting phase with a lower T_c is characteristic of samples Nos. 1, 3, 5, 10 and 16. Samples containing more than 0.5 moles of ruthenium per mole of yttrium loose their superconductivity.

Thermal cycling of samples with high T_c results in hysteresis for practically all of these sintered samples after the first cycle (293–77 K and 77–180 K), the T_c being 94 K on cooling and 107 K on heating. No hysteresis arises during further cycling; T_c first increases, then gradually decreases (see Figure 1) before becoming stable at 94 K after the 17th cycle. Storing the samples in liquid nitrogen (6), as well as thermal cycling (7), is known to increase T_c, which may be caused by some micro- or macrostructural phase transformation up to the quasi-equilibrium state.

Samples with T_c higher than the liquid nitrogen temperature were studied by X-ray phase analysis. Samples containing 0.1–0.7 moles of ruthenium (per mole of yttrium) appeared to be two phase (Figure 2a), the $YBa_2Cu_3O_{7-\delta}$ phase was superconducting, while the other ruthenium-containing phase exhibited semiconducting behaviour. In the sample with a ruthenium content of 0.8 moles only the semiconducting phase was found to be present. Unit cell parameters are listed in Table II. When the ruthenium content was above 0.9 moles (per mole of yttrium) the sample was multiphase. However, the samples are superconducting, see Table III when the

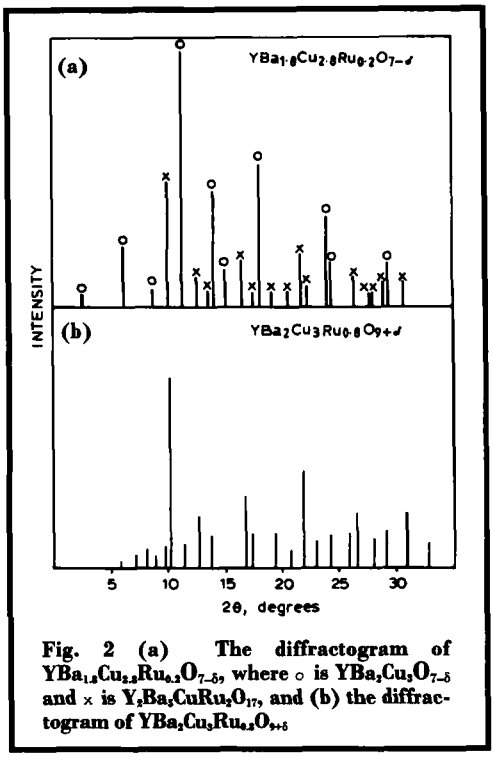

Fig. 2 (a) The diffractogram of $YBa_{1.8}Cu_{2.8}Ru_{0.2}O_{7-\delta}$, where ○ is $YBa_2Cu_3O_{7-\delta}$ and × is $Y_2Ba_5CuRu_2O_{17}$, and (b) the diffractogram of $YBa_2Cu_3Ru_{0.2}O_{9+\delta}$

ratio of the intensities of the main peaks on the X-ray diffraction pattern of the sample under study of the superconducting, I_{sc}:I_{nsc} non-superconducting (semiconducting) phases, is above 0.485. This provides evidence for the existence of a "percolation limit" in the superconducting phase contents, below which superconductivity is not observed. This may be interpreted in terms of the infinite three-dimensional cluster (8) of Josephson junctions (9).

Using X-ray microanalysis the composition of the semiconducting ruthenium-containing phase, for all samples with ruthenium contents less than 0.9 moles was found to be $Y_2Ba_5CuRu_2O_x$. But in the sample with ruthenium content of 0.8 moles, only this phase was found to be present. The compound is brown in colour and its melting point was found by thermal gravimetric analysis to be 1090°C. The valence states of ruthenium and the other elements were examined by X-ray photoelectron spectroscopy (XPS). The peaks of the elements contained in the Y-Ba-Cu-Ru-O_x system are shown in the wide-scan spectrum, see Figure 3, where data for all the systems under investigation are summarised.

The oxidation state of the ruthenium on the surface of Y-Ba-Cu-Ru-O samples can be evaluated from the dependence of $E_b(Ru3d_{5/2})$, where E_b is the binding energy, on n (10), where n is the coefficient in RuO_n. However, before the localisation of the $Ru3d_{5/2}$, and the Ru3d line intensities, it is necessary to distinguish between the contribution from the Ru3d and C1s lines. The carbon may result from surface contamination, residual gases in the vacuum system, non-

Table II

Measured Values of the d Spacing and Intensities, I, of the Major Peaks on X-ray Diffraction Patterns of Superconducting $YBa_2Cu_3O_{7-\delta}$(I) and Semiconducting Ruthenium Phases (II)

(I)		(II)	
d,nm	I, per cent	d,nm	I, per cent
0.2836	100	0.2735	100
0.2700	43	0.2333	40
0.2076	33	0.1580	31
0.1470	19	0.387	25
0.1315	16	0.1363	18

Table III

Parameters of the Ruthenium-Containing Samples

Sample number	Composition	T_c(R),K		I_{ac}(0.2836 nm) / I_{nac}(0.2735 nm)
		T_{oo}	T_c	
1	$YBa_{1.8}Cu_{2.9}Ru_{0.1}O_{7-\delta}$	97	96.5	5.65
2	$YBa_{1.8}Cu_{2.9}Ru_{1.5}O_{7-\delta}$	97	95	4.4
3	$YBa_{1.8}Cu_{2.8}Ru_{0.2}O_{7-\delta}$	95	92	2.18
4	$YBa_{1.8}Cu_{2.9}Ru_{0.2}O_{7-\delta}$	97	96.5	1.79
5	$YBa_2Cu_{2.7}Ru_{0.3}O_{7-\delta}$	96	95	1.4
6	$YBa_2Cu_{2.5}Ru_{0.5}O_8$	90	89	1.135
7	$YBa_2Cu_{2.6}Ru_{0.4}O_{7-\delta}$	99	94	0.86
8	$YBa_{1.8}Cu_3Ru_{0.4}O_{7+\delta}$	97	96	0.68
9	$YBa_{1.8}Cu_3Ru_{0.5}O_{8+\delta}$	94	93	0.485
10	$YBa_{1.8}Cu_3Ru_{0.7}O_8$	–	–	0.39
11	$YBa_2Cu_3Ru_{0.7}O_{9+\delta}$	–	–	0.295
12	$YBa_2Cu_3Ru_{0.8}O_{9+\delta}$	–	–	single-phase
13	$YBa_2Cu_3Ru_{0.9}O_{10+\delta}$	–	–	multiphase

reacting part of the starting powders, and so on, which overlap in the XPS spectrum for Y-Ba-Cu-Ru-O samples, Figure 4. For this purpose the intensity of a non-overlapping line, Ru3*p*, and the ratio Ru3*p*:Ru3*d* have been determined for RuO_2 powder. The Ru3*p*:Ru3*d* ratio measured coincided with the value calculated to an accuracy of 3 per cent (11). In the case of RuO_2, it was not difficult to estimate the separate Ru3*d* and C1*s* contributions, since the most intensive peak, Ru3$d_{5/2}$, did not overlap with the C1*s* spectrum, Figure 4.

The Ru3$d_{5/2}$ peak position (284.7 eV) for two Y-Ba-Cu-Ru-O samples provides evidence for the high oxidation state of the ruthenium atoms. The value for E_b(Ru3$d_{5/2}$) is 283.2–283.6 eV for RuO_2, depending on the calibration method (10). Such high values of E_b(Ru3$d_{5/2}$) were obtained in the Y-Ba-Cu-Ru-O samples for which the values of E_b(O1*s*) and E_b(Cu2$p_{3/2}$) were usual, that is,

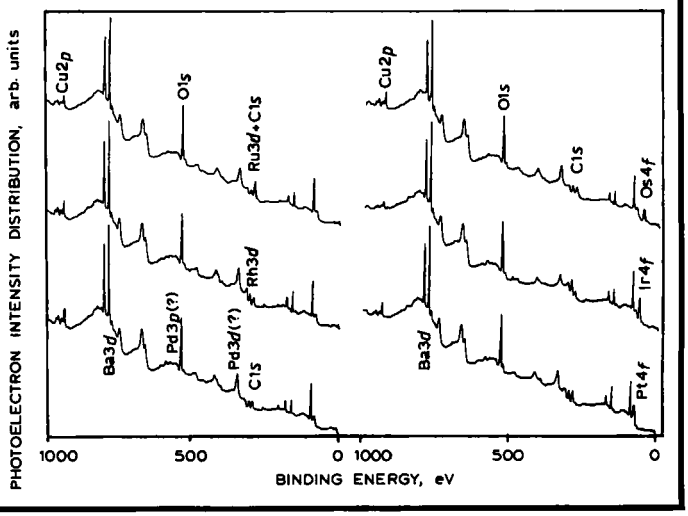

Fig. 3 Wide-scan X-ray photoelectron spectra of the Y-Ba-Cu-M-O samples, where M is a platinum group metal (see Table IV), (showing photoelectron intensity distribution against binding energy)

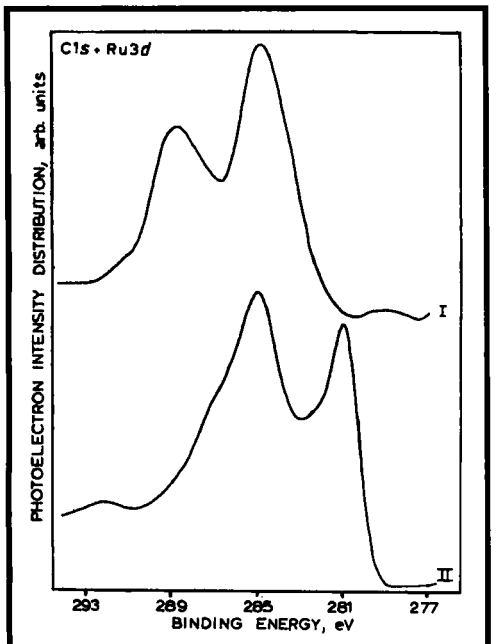

Fig. 4 X-ray photoelectron spectra of $YBa_2Cu_{2.7}Ru_{0.3}O_{7-\delta}$ (I) and RuO_2 (II), within the Ru3*d* + C1*s* range

coincident with those for $YBa_2Cu_3O_{7-\delta}$ (12–14). Consequently, the oxidation state of ruthenium in the compositions under consideration is high, Ru^{8+} being most probable. Therefore, the final composition of the ruthenium phase may be represented as $Y_2Ba_3CuRu_2O_{17}$ (3, 15), a compound of sufficient stability under high vacuum.

In Table IV the bulk and surface compositions of the samples are given, the surface composition being determined from the following formula:

$$[C_x] = 100 \cdot \frac{I_x}{\sigma_x}\left\{\sum_j\left(\frac{I_j}{\sigma_j}\right)\right\}^{-1}$$

where $[C_x]$ is the concentration (in atomic per cent) of element x, I is the integral intensity of the analytical lines and σ is the photo-ionisation cross-section. The summation was performed along the analytical lines for the metals. A comparison of the bulk and surface compositions showed that the surface of all the samples in the Y-Ba-Cu-M-O system, where M is a platinum group metal, was barium enriched, as in the case of $YBa_2Cu_3O_{7-\delta}$. (The $Ba3d_{5/2}$ line of relatively low kinetic energy, about 470 eV, was taken to be an analytical one). The coefficient, γ, where $\gamma_x = [C_x]^{sur}/[C_x]^{bulk}$, is presented in Table IV for the platinum group metals which, in our opinion, are the most interesting. (Values of $[C_x]^{sur}$ were obtained by XPS, while values of $[C_x]^{bulk}$ were obtained by chemical analyses).

The elements of the platinum group may be divided into three sub-groups: ruthenium and iridium, with γ much greater than 1, constitute the first sub-group; the second sub-group contains platinum, rhodium and osmium, while palladium is the only representative in the third sub-group with $\gamma = 0$, even at very high palladium concentrations.

Considerable enrichment of the surface by a modifying agent may take place when it is not incorporated into the lattice of the main crystal phase. When $YBa_2Cu_3O_{7-\delta}$ is the main phase, the presence of a platinum group metal, M, does not decrease the T_c value, as shown by the measurements of the temperature dependence of the magnetic susceptibility, and as observed for the ruthenium containing samples.

The $YBa_2Cu_3O_{7-\delta}$ + Rhodium System

Like ruthenium, the other platinum group metals are catalysts for the synthesis of $YBa_2Cu_3O_{7-\delta}$, which is shown by a faster reaction, the absence of a "green" phase, (Y_2BaCuO_5) and a decrease in the reaction temperature.

The $YBa_2Cu_3O_{7-\delta}$ + rhodium system is very similar to that containing ruthenium, that is, its T_c is dependent on the ratio of the components. The presence of only one rhodium-containing phase, $Y_3Ba_{10}CuRh_3O_x$, is characteristic of the system (X-ray microanalysis data). The results of the XPS study of this compound are presented below, its wide-scan spectrum being shown in Figure 3.

The $Rh3d_{5/2}$ peak, which is the most frequently used analytically for rhodium compounds, is easy to distinguish in the XPS spectrum of the Y-Ba-Cu-Rh-O composition. Its position at 309.4 eV is evidence for rhodium being in the 3+ oxidation state in the oxide matrix (16). It should be noted that the "typical" value of $E_b(Rh3d_{5/2})$ for

Table IV

Bulk and Surface Compositions of Samples from the Y-Ba-Cu-M-O System, where M is a Platinum Group Metal

No.	Sample	Composition, at.%								γ_M
		Bulk				Surface				
		Y	Ba	Cu	M	Y	Ba	Cu	M	
1	$YBa_2Cu_{2.7}Ru_{0.3}O_x$*	17	33	45	5	19	42	31	8	1.6
2	$YBa_2Cu_{2.2}Ru_{0.8}O_x$	17	33	37	13	23	41	13	23	1.8
3	$YBa_2Cu_3Rh_{0.7}O_x$*	15	30	45	10	24	38	28	10	1.0
4	$YBa_2Cu_3Pd_{0.05}O_x$	17	33	49	1	24	38	38	0	0
5	$YBa_2Cu_3Pd_{0.3}O_x$*	16	32	48	4	18	39	43	0	0
6	$YBa_2Cu_3Pd_{0.3}O_xCl_y$**	16	32	48	4	16	46	38	0	0
7	$YBa_2Cu_3Pd_{0.8}O_x$	15	30	44	11	20	48	32	0	0
8	$YBa_2Cu_3Pd_2O_x$	12	25	37	25	23	26	25	26	1.0
9	$YBa_2Cu_3Os_{0.7}O_x$*	15	30	45	10	20	40	30	10	1.0
10	$Y_2Ba_3Cu_2OsO_{10+\delta}$	25	37	25	12	14	46	32	6	0.5
11	$YBa_2Cu_3Ir_{0.7}O_x$*	15	30	45	10	25	42	16	17	1.7
12	$YBa_2Cu_3Pt_{0.7}O_x$*	15	30	45	10	23	40	23	13	1.3
13	$Y_2Ba_3Cu_2PtO_{10}$	25	37	25	12	32	36	21	11	0.9

**y<0.1

*The wide-scan X-ray photoelectron spectrum of the sample is shown on Figure 3

the Rh^{3+} complexes is 310.7 eV. However, the value of 308.9 eV has been reported elsewhere for the Rh_2O_3 oxide (17).

Thus, the formal oxidation state of the rhodium modifying agent in the Y-Ba-Cu-Rh-O samples is 3+, however, the positive charge on the rhodium atom in the sample studied is noticeably higher than for Rh_2O_3. These data allowed the refined formula of the rhodium phase to be determined as $Y_3Ba_{10}CuRh_3O_{20}$.

The $YBa_2Cu_3O_{7-\delta}$ + Palladium System

The modification of the $YBa_2Cu_3O_{7-\delta}$ system by palladium of more than 0.001 atomic per cent results in the complete loss of superconductivity (18, 19). In subsequent literature palladium has been shown to substitute for copper in the superconductor lattice, forming $YBa_2Cu_{2.5}Pd_{0.5}O_7$ (20). The absence of palladium on the surface of the Y-Ba-Cu-Pd-O samples with high palladium contents is evidence of this (Table IV, XPS data), the copper content being somewhat increased (when compared with the other samples containing the same amount of modifying agent M).

Of the samples in the Y-Ba-Cu-Pd-O system studied, only No. 8 had sufficient surface concentration of palladium to differentiate the Pd3$d_{5/2}$ peak from the XPS background noise (Table IV). The E_b(Pd3$d_{5/2}$) value of 336.6 eV is evidence that the palladium oxidation state in the undersurface layer is 2+. For PdO the value of E_b(Pd3$d_{5/2}$) is 336.5 eV (21), which is almost the same as obtained in our measurements.

Nevertheless, it seems unreasonable to expect the oxidation state of the promoting element to be the same as in sample No. 8.

By means of X-ray microanalysis three new phases were detected in the $YBa_2Cu_3Pd_2O_{8.5}$ sample annealed at 900°C.

The $YBa_2Cu_3O_{7-\delta}$ + Osmium System

This system was studied as thoroughly as that of ruthenium. A series of $YBa_2Cu_3Os_xO_y$ samples (with x = 0.1–1.0) was synthesised according to the procedure described in (3).

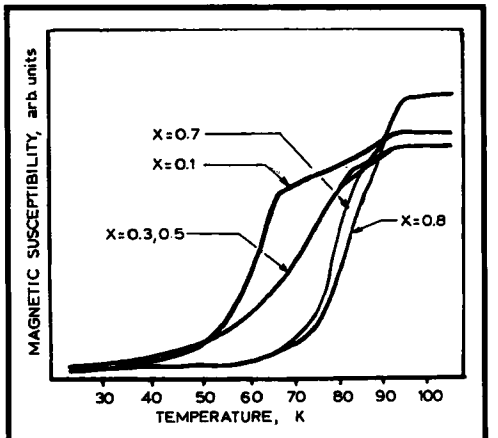

Fig. 5 The temperature dependence of magnetic susceptibility in $YBa_2Cu_3Os_xO_y$, where x = 0.1–0.8

All the samples, are multiphase compounds. In samples with x = 0.1–0.8 two superconducting phases are distinguishable, one having T_c = 93 K, while the T_c values of the other phase may vary from 62 K to 83 K (Figure 5). Samples with x = 0.9 and x = 1.0 are not superconducting. The XPS method was used to determine the oxidation state of the osmium (see Figure 3 for the wide-scan spectrum). Since there is no information in the literature on the dependence of the most intensive osmium peak, $4f_{7/2}$, on the osmium oxidation state, our data in Figure 6 may be of interest. The E_b(Os $4f_{7/2}$) values were found to be 53.5 and 54.3 eV for samples with x = 0.7 and 1.0, respectively, which correspond to Os^{4+} (x = 0.7) and Os^{5+} (x = 1.0). The osmium $4f$ line shape (a larger half-width) is evidence for the presence of states other than the main states of the osmium atoms in the sample under study (Figure 7).

X-ray phase analysis showed that samples with x = 0.1–0.8 consisted of the main phase: $YBa_2Cu_3O_{7-\delta}$ (*Pmmm*, a = 0.3882, b = 0.3891, c = 1.1688 nm for the sample with x = 0.7), and an admixture phase: $BaOsO_3$ (In3m, a = 0.935 nm) (see Figure 8). Copper oxide and unidentified compounds with diffraction peaks at d = 0.4833 and 0.4187 nm were also detected among the admixtures.

The data from XPS and X-ray phase analysis may lead to the conclusion that the compound with four-valent osmium, $BaOsO_3$, is formed in samples with x = 0.1–0.8, see Table V.

The non-superconducting samples, with x = 0.9 and 1.0, consist of two unknown osmium phases (as the main components) and a small amount of $YBa_2Cu_3O_{7-\delta}$, Y_2BaCuO_5, $BaCuO_2$

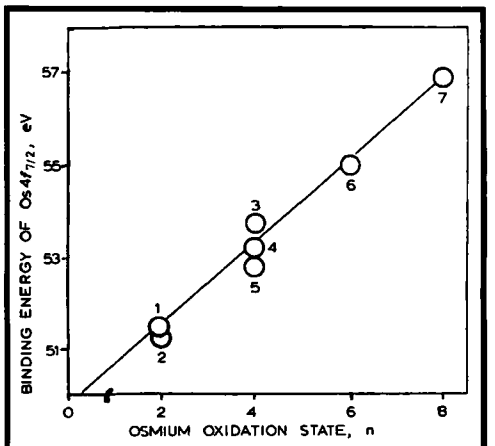

Fig. 6 The dependence of the binding energy E_b(Os$4f_{7/2}$) on the osmium oxidation state n, in metal complexes. The E_b(Os$4f_{7/2}$) values for complex 2 - $K_4[Os(CN)_6].4H_2O$ and 5 - $[OsCl_4(PMe_2Ph)_2]$ are taken from (22) and (23), respectively. 1 - $[OsN_2(NH_3)_2Cl_2]$; 3 - K_2OsCl_6; 4 - K_2OsBr_6; 6 - $K[OsNBr_4(H_2O)].H_2O$ and 7 - $K[OsO_3N]$

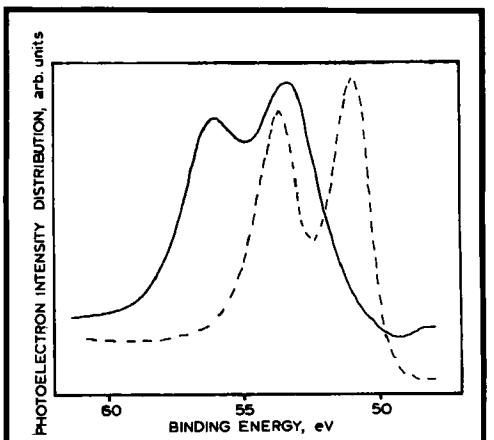

Fig. 7 X-ray photoelectron spectra of the $YBa_2Cu_3Os_{0.7}O_x$, solid line, and metallic osmium, dotted line

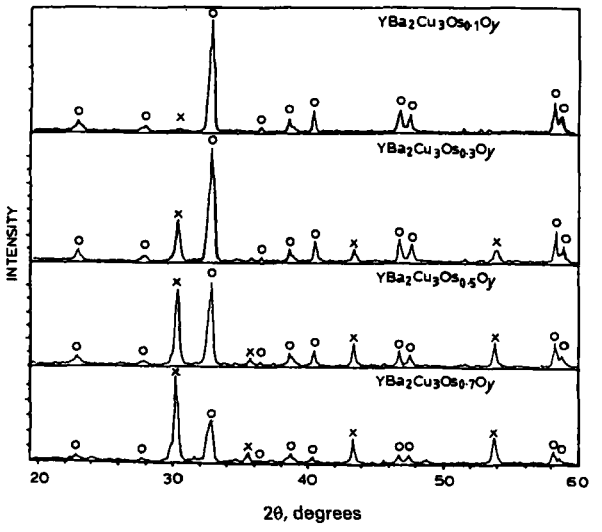

Fig. 8 X-ray powder diffraction patterns of $YBa_2Cu_3Os_xO_y$ for osmium content x = 0.1–0.7, where ○ is $YBa_2Cu_3O_{7-\delta}$ and × is $BaOsO_3$

and $Y_2Cu_2O_5$. The unknown phases were identified as $Y_2Ba_3Cu_2OsO_x$ and $YBa_3Cu_4Os_{0.1}O_x$ by X-ray microanalysis. Since the oxidation state of osmium in samples with x = 0.9 and 1.0 is 5+ (XPS data), the phases may be presented as $Y_2Ba_3Cu_2OsO_{10.5}$ and $YBa_3Cu_4Os_{0.1}O_{8-\delta}$. Attempts to synthesise the phase $Y_2Ba_3Cu_2OsO_{10.5}$ in its pure form were a failure and gave a mixture of compounds, such as Y_2BaCuO_5 (Pbnm; a = 0.7131, b = 1.2164, c = 0.5657 nm), $BaCuO_2$ (Im3m, a = 1.8294 nm), and $Y_2Cu_2O_5$. The other diffraction peaks in the XRD pattern of this sample were attributed to the $Y_2Ba_3Cu_2Os(V)O_{10.5}$ phase (Table VI). The synthesis of the other osmium phase, $YBa_3Cu_4Os_{0.1}O_{8-\delta}$, was not a success either. X-ray phase analysis showed the presence of $YBa_2Cu_3O_{7-\delta}$, $BaCuO_2$ and Y_2BaCuO_5. The XRD data on the fourth phase are given in Table VI. They were thought to belong to $YBa_3Cu_4Os_{0.1}(V)O_{8+\delta}$.

Table V
XRD Data of $BaOsO_3$ (24) and the Osmium Phase in $YBa_2Cu_3Os_{0.7}O_y$

Obtained		Ref. 24	
d, nm	I, %	d, nm	I, %
0.2957	100	0.2961	100
0.2090	46	0.2078	10
0.1706	52	0.1708	50
0.1321	18	0.1325	50

The $YBa_2Cu_3O_{7-\delta}$ + Iridium System

This system is a close analog to the ruthenium and rhodium systems. The dependence of T_c on the ratio of the initial elements was also similar to

Table VI
Data on the X-ray Phase Analysis of $Y_2Ba_3Cu_2OsO_{10.5}$ (I) and $YBa_3Cu_4Os_{0.1}O_{8+\delta}$ (II)

(I)		(II)	
d_{obs}, nm	I,%	d_{obs}, nm	I,%
7.998	25	0.4810	7
4.800	100	0.4132	5
4.132	30	0.3101	9
4.004	20	0.3013	20
3.718	25	0.2953	100
2.901	10		
2.346	50		

that of the ruthenium system (see Table I). X-ray phase analysis and X-ray microanalysis detected only one iridium compound in the system, which appeared to be $Y_3Ba_6CuIr_6O_x$, with a face centred cubic F-cell (a = 0.8341 nm).

According to the XPS data the $E_b(Ir4f_{7/2})$ value for the Y-Ba-Cu-Ir-O sample is 63.2 eV. It should be noted that the $E_b(Ir4f_{7/2})$ values obtained for K_3IrCl_6 and K_2IrCl_6 complexes are 62.6 and 63.7 eV, respectively, (16) and the $E_b(Ir4f_{7/2})$ value for the main state of the Ir/Al_2O_3 catalyst stored in air is 62.5 eV (25), and it was thought that the main iridium state on the catalyst surface was Ir^{4+} (25). Therefore it may be expected that the Ir^{4+} oxidation state is highly probable in the Y-Ba-Cu-Ir-O system, at least in the undersurface layer. It is also noteworthy that the Ir4*f* line of the sample is rather narrow; consequently iridium is included in the composition of only one compound on the surface, which agrees with the X-ray microanalysis data. A high coefficient of surface enrichment, γ, with iridium may lead to the supposition that the size of the iridium containing particles is smaller than that of the main phase present, namely $YBa_2Cu_3O_{7-\delta}$.

Thus, from the above data the iridium compound can be represented as $Y_3Ba_6CuIr_6O_{23.5}$.

The $YBa_2Cu_3O_{7-\delta}$ + Platinum System

This system has been studied in the greatest detail, and was considered in (2), and results of the XPS study are described here.

The main state of platinum in samples of the Y-Ba-Cu-Pt-O system was found to be Pt^{4+}, since measurements gave $E_b(Pt4f_{7/2})$ = 74.4 eV, which is closer to 74.5 eV for PtO_2 than to 73.7 eV for PtO (26). However, considerable shoulders were seen on the Pt4*f* spectrum in the region of higher binding energies (Figure 9). At present it is difficult to find an unequivocal explanation of this phenomenon, although we considered two hypotheses: first, the influence of the $K\alpha_{3,4}$ satellite of the Ba4*d* line and second, the presence of platinum ions in an oxidation state higher than 4+.

A careful examination of the spectral site of samples not containing platinum shows that the $K\alpha_{3,4}$ satellite of the Ba4*d* line does overlap with the Pt4*f* spectrum. The line shape of the Pt4*f* spectrum is very dependent on the Pt:Ba ratio, so that at low values of the ratio the height of the $Pt4f_{5/2}$ peak may be greater than that of the $Pt4f_{7/2}$ peak. It should also be noted that the shape of the $K\alpha_{3,4}$ satellite of the Ba4*d* line is rather smooth, and it seems impossible to explain the shoulder in the spectrum Pt4*f* (marked * in Figure 9) only by means of the contribution of this satellite. We now attribute this effect to the presence of Pt^{6+}. However, we have not succeeded in observing this effect on the spectrum of the known $Y_2Ba_3Cu_2PtO_{10}$ (27), which is evidence for the presence of as yet undetected phases with Pt^{6+} in the $YBa_2Cu_3O_{7-\delta}$ + platinum system.

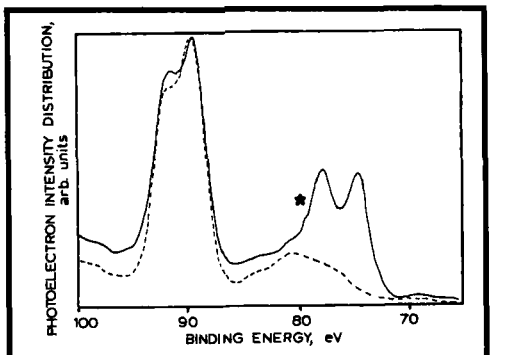

Fig. 9 X-ray photoelectron spectra of $YBa_2Cu_3O_{7-\delta}$, dashed line, and $YBa_2Cu_3Pt_{0.7}O_x$, solid line, within the Ba4d + Pt4f range

Conclusion

The following generalised conclusions have been made from the data considered here:

Superconductivity in $YBa_2Cu_3O_{7-\delta}$ + M, where M is a platinum group metal, depends on the amount of M in the system, the lowest values being characteristic of systems with palladium, which substitutes for copper in the superconductor structure. The highest amounts of M have been found for the osmium system, barium osmate being formed in this case. All platinum metals form new non-superconducting (semiconducting) phases, listed in Table VII.

As seen from Table VII, ruthenium exhibits the highest oxidation state of 8+ in this complicated system, the existence of a Pt^{6+} compound

Table VII

Composition	Metal valency	X-ray data	References
$YBa_5CuRu_2O_{17}$	+8		herein
$Y_3Ba_{10}CuRhO_{20}$	+3		herein
Y_2BaPdO_5	+2	tetragonal, P4/mbm, a = 0.6523, c = 0.5831 nm	32
Nd_2BaPdO_5	+2	as above	32
$YBa_2Cu_{2.5}Pd_{0.5}O_7$	+2	orthorhombic, Pmmm, a = 0.3841, b = 0.3883, c = 1.1617 nm	20
$YBa_3Cu_5Pd_3O_{10.5}$	+2		herein
$YBa_3Cu_8Pd_3O_{20}$	+2		herein
$Y_6Ba_5Cu_3Pd_3O_{20}$	+2		herein
$Y_2Ba_3Cu_2OsO_{10.5}$	+5		herein
$YBa_3Cu_4Os_{0.1}O_{8+\delta}$	+5		herein
$YBa_6CuIr_6O_{23.5}$	+4	cubic, face-centred, F-cell, a = 0.8341 nm	herein
$YBa_2Cu_3Pt_{0.7}O_{7+\delta}$	+4, +6		herein
$Y_2Ba_3Cu_2PtO_{10}$	+4	monoclinic, C2/c, a = 1.2518, b = 0.5828, c = 0.7362 nm	herein 2,27,28,29
$Ho_2Ba_3Cu_2PtO_{10}$	+4	monoclinic, C2/m, a = 1.2516, b = 0.5813, c = 0.7350 nm	29
$Y_2Ba_2CuPtO_8$	+4	orthorhombic, Pnma, a = 1.3191, b = 0.5680, c = 1.0301 nm	30, 31
$Er_2Ba_2CuPtO_8$	+4	rhombic, Pcmn, a = 1.0287, b = 0.5659, c = 1.3157 nm	31
$Ho_2Ba_2CuPtO_8$	+4	as above	31
Nd_2BaPtO_5	+2		32
$YBa_{2.3}Cu_{0.2}PtO_6$	+2, +4	pseudocubic, perovskite, a = 1.2316 nm	33
$Y_2(Ba, Sr)_2SrPtCu_2O_{10}$	–	centrosymmetric, C2/m a = 1.2316 nm	34
$La_{1.48}Ca_{40}Ba_{.87}Cu_{2.8}Pt_{20}O_y$	–		35
$ErBa_{1.03}Cu_{0.77}Pt_{0.46}O_{4.34}$	–	rhombic, Pcmm, a = 1.0287, b = 0.5655, c = 1.3157 nm	36
$Ba_4Pt_{1+x}Cu_{2-x}O_{9-y}$ (x<0.5)	–	hexagonal, a = 0.5803, c = 1.8450 nm	37
$La_{1.5}Sr_{0.5}Cu_{0.75}Pt_{0.25}O_4$	–	Abma, a = 0.5416, b = 0.5416, c = 1.2943 nm	38
$LnBa_2Cu_{3-x}Pt_xO_{9-\delta}$(Ln = Sc, Y, Pr, Nd, Tb, Tu, Yb, Lu)		hexagonal, a = 1.0050–1.0078, c = 0.8320–0.8352 nm	39
$Er_3Ba_8Pt_4O_{17.5}$	–	Pm3m, a = 0.83441 nm	40
$Yb_3Ba_8Pt_4O_{17.5}$	–	Pm3m, a = 0.83145 nm	40
$Tm_3Ba_8Pt_4O_{17.5}$	–	Pm3m, a = 0.83296 nm	40
$Sc_3Ba_8Pt_4O_{17.5}$	–	cubic, Pm3m, a = 0.81531 nm	41
$Tb_3Ba_8Pt_4O_{17.5}$	–	cubic, Pm3m, a = 0.8571 nm	41

is assumed, the oxidation state of osmium is 5+, and rhodium, iridium and palladium are all in their standard valence states. In addition, ruthenium, rhodium, and iridium form only one compound with the Y-Ba-Cu-O system, while the platinum and palladium systems are the most diverse. The ability to form perfect crystals (particularly iridium, platinum, osmium), their

semiconducting properties, ease of synthesis and stability in air and vacuum make these compounds quite possibly suitable for engineering and chemical technology (as catalysts for oxidation and burn-off of waste gases, in fuel cells and for semiconducting techniques).

Readers who wish to receive a copy of XRD data on $Y_3Ba_{10}CuRh_3O_{20}$, $YBaCu_5Pd_3O_{10.5}$, $YBa_8Cu_8Pd_3O_{20}$, $Y_6Ba_5Cu_3Pd_3O_{20}$ and $Y_3Ba_6CuIr_6O_{23.5}$ established during these investigations should send their request to Dr. Yu. M. Shul'ga, Institute of Chemical Physics, Chernogolovka, 142432, Moscow Region, Russia.

References

1 J. D. Bednorz and K. A. Muller, *Z. Phys. B, Condens. Mater.*, 1986, **64**, 189

2 E. F. Maher, *Platinum Metals Rev.*, 1991, **35**, (1), 2

3 E. N. Izakovich, A. T. Mailybaev, G. D. Sokolovskaya, Yu. M. Shul'ga, V. I. Rubtsov, Yu. M. Korolev, V. N. Spector and M. L. Khidekel, *Phys. Status Solidi (a)*, 1991, **124**, 525

4 B. R. James, "Homogeneous Hydrogenation", Wiley-Intersci. Publ., New York, 1973

5 I. E. Graboi, A. P. Kaul and Yu. G. Metlin, "Itogi Nauki i Tekhniki. Ser. Khimiya Tverdogo Tela" (Russ.), 1988, **6**, 37

6 D. H. Matthew, A. Bailey, R. A. Vaile, G. J. Russell and K. N. Taylor, *Nature*, 1987, **328**, 786

7 H. D. Tostarndt, M. Calffy, A. Freimuta and D. Wohllenben, *Solid State Commun.*, 1989, **69**, 911

8 M. Nunez Requeiro, P. Esquenazi, M. A. Izbizky, C. Duran, D. Castello, T. Luzuriaga and G. Nieva, *Physica*, 1988, **C153**, 1016

9 S. R. Shenoy, *Physica*, 1988, **B152**, 72

10 C. D. Wagner, W. H. Riggs, L. E. Davis, J. F. Moulder and H. Mullernerg, eds., "Handbook of X-Ray Photoelectron Spectroscopy", Perkin-Elmer Corp., Minnesota, 1979, p. 190

11 J. H. Scofield, *Livermore Lab. Rep.*, UCRL-51326, 1973

12 N. Nuckel, J. Fink, B. Renkel, D. Ewert, C. Politis, P. J. W. Weijs and J. C. Fuggle, *Z. Phys.*, 1987, **B67**, 1

13 H. Ihara, M. Hirabayashi, N. Terada, Y. Kimura, K. Sensaky, A. Akimoto, K. Bushida, F. Kawashima and R. Uzuha, *Jpn. J. Appl. Phys.*, 1987, **26**, L460

14 P. Steiner, V. Kinsinger, I. Sander, B. Siegwart, B. Hufner, C. Politis, R. Hoppe and H. P. Muller, *Z. Phys.*, 1987, **67**, 487

15 Yu. M. Shul'ga, V. I. Rubtsov, E. N. Izakovich and Yu. G. Borod'ko, *Surface (Russ.)*, 1991, **6**, 121

16 V. I. Nefedov, "X-Ray Photoelectron Spectroscopy of Chemical Compounds" (Russ.), Khimiya, Moscow, 1984, p. 284

17 M. N. Firsov, V. I. Nefedov and E. P. Domashevskaya, *J. Struct. Chem. (Russ.)*, 1979, **20**, 49

18 Y. Nishii, S. Moriya and S. Tokunaga, *Phys. Lett., A*, 1987, **126**, 55

19 T. J. Wagener, Y. Gao, I. M. Vitomirov, C. M. Aldao, J. J. Joyce, C. Capasso and J. H. Weaver, *Phys. Rev.* B, 1988, **38**, 232

20 G. Ferrey, A. LeBail, Y. Laligant, M. Merkieu, B. Raveau, A. Suplice and R. Tournier, *J. Solid State Chem.*, 1988, **13**, 610

21 K. S. Kim, A. G. Goosmann and N. Winograd, *Anal. Chem.*, 1974, **46**, 197

22 V. I. Nefedov, N. M. Spitsyn and Ya. V. Salyn, *Koord. Khimiya (Russ.)*, 1975, **1**, 1618

23 G. J. Leigh and W. Bremser, *J. Chem. Soc., Dalton Trans.*, 1973, 1216

24 A. M. T. Bell, *Supercond. Sci. Technol.*, 1990, **3**, 55

25 A. V. Bulatov, T. P. Geidei, S. N. Ustritskii, I. Ya. Turaev, M. L. Khidekel, Yu. M. Shul'ga and N. M. Yaroshenko, *Kinet. Katal. (Russ.)*, 1988, **29**, 238

26 K. S. Kim, N. Winograd and R. E. Davis, *J. Am. Chem. Soc.*, 1971, **93**, 6296

27 E. A. Genkina, O. K. Melnikov, A. B. Bykov and B. A. Maksimov, *Kristallografiya*, 1989, **34**, 1426

28 G. Calestani, C. Rizzoli and G. D. Andreotti, *Solid State Commun.*, 1988, **66**, 223

29 U. Geiser, L. C. Porter, H. H. Wang, J. A. Allen and J. M. Williams, *J. Solid State Chem.*, 1988, **73**, 243

30 J. S. Swinnea and H. Steinfink, *Acta Cryst.*, 1987, **C43**, 2436

31 N. Toyota, P. Koorevaar, J. van der Berg, P. H. Kes, T. Shisido, Y. Saito, N. Kuroda, K. Ukei and J. Sasaki, *J. Phys. Condens. Matter*, 1989, **1**, 3721

32 Y. Laligant, G. Ferrey, M. Hervieu and B. Raveau, *Eur. J. Solid State Inorg. Chem.*, 1988, **25**, 111

33 P. Gouzerh, F. Robert, J. Gouzerh and H. Makram, *J. Cryst. Growth*, 1990, **102**, 1059

34 M. Hiorth, *Acta Chem. Scand.*, 1988, **42A**, 727

35 U. Amador, E. Moran, M. Alario-Franco, A. Vegas, M. Martinez-Ripoli, J. Ibanez and J. B. Torrance, *Physica C*, 1989, **C162**, 8731

36 I. Shishsido, T. Fukuda, N. Toyoto, K. Ukei and T. Sasaki, *J. Cryst. Growth*, 1987, **85**, 599

37 Z. Chen, Y. Qian, Y. Wu, D. Sun, R. Lin, T. Cheng, L. Niu, G. Zhou, Z. He, J. Xia, Y. Zao and Q. Zhang, *J. Cryst. Growth*, 1989, **94**, C277

38 H. K. Muller-Buschbaum and A. Teichert, *J. Less-Common Met.*, 1989, **155**, 9

39 Y. Qian, Z. Chen, T. Chen, G. Pan, Q. Zhang, J. Xia, Y. Zhao, Z. He, G. Zhow, T. Cheng and L. Niu, *Mater. Res. Bull.*, 1988, **23**, 119

40 W. Gutau and H. Muller-Buschbaum, *Z. Anorg. Allg. Chem.*, 1990, **584**, 7

41 W. Gutau and H. Muller-Buschbaum, *J. Less-Common Met.*, 1990, **159**, 223